

**LEMP2020-XXXX**

## **FEASABILITY STUDY FOR AN ULTRASONIC SENSOR FOR MONITORING WHEEL FLANGE CONTACT**

**First Author, Second Author**  
University of Sheffield, Sheffield, UK

**Third Author, Fourth Author**  
ASME, New York, NY

### **ABSTRACT**

If the contact between the wheel and rail occurs at the flange, a high degree of slip is inherent. This can result in excessive wear and the potential for rolling contact fatigue cracking. Multi-body dynamics software is useful for predicting the bogie and track characteristics that may lead to flange contact occurring. However, there is a shortage of experimental tools available to validate such models or to assist in vehicle and track condition monitoring.

In this study, the feasibility of a new approach is investigated. The method is based on an ultrasonic sensor mounted on the wheel. The concept is that the sensor emits an ultrasonic pulse which is designed to impinge on the wheel flange. If there is no contact the pulse is fully reflected back at the flange and picked up by the same sensor. If flange contact takes place, a proportion of the pulse amplitude will be transmitted into the rail. The signal reflected back to the sensor is therefore reduced. The amount by which this signal reduces indicates how much flange contact occurs.

Test specimens were cut from sections of wheel and rail, and a 2MHz ultrasonic contact transducer was bonded onto the wheel in a position best suited to detect the flange contact. The specimens were pressed to together in a bi-axial loading frame to generate differing degrees of head and flange contact. The reflected signal was monitored as the normal and lateral loads were varied. It proved possible not only to detect the onset of flanging, but also to record a signal that varied monotonically with both normal and lateral applied load. A map of reflected ultrasound against the applied loading is presented.

### **INTRODUCTION**

The wheel/rail contact is critical to the successful operation of a railway network. Contact occurs mainly at the wheel tread/rail head and wheel flange/rail gauge corner. Contact conditions are more severe in the latter, which occurs mainly in curves. The contact is small and supports large loads, therefore high contact stresses are generated. These combined with the slip in the contact are primarily responsible for driving the processes that lead to wheel and rail damage, whether it be by deformation, wear or a fatigue process [1].

Effective management of the wheel/rail contact is an important aspect of rail infrastructure operations. All the influencing factors have to be taken into account as they interact closely.

There is clearly a need for information about the wheel/rail contact interface in term of position, area, and contact stresses. This is particularly important when problems such as wear and RCF may occur. There are several analytical and numerical models for analysing the wheel/rail contact. However, there are few experimental techniques for measuring contacts. Pressure sensitive films have been used to determine the extent of contacts [2]. However, these change the nature of the contact and therefore suitable only as an indicator. Dynamic wheel/rail contact area measurements have been taken using low-pressure air passing through 1 mm diameter holes drilled into the rail head [3]. The pressure variations caused as holes were blocked by passing wheels were monitored and areas determined. This, however, can only give very limited spatial data.

An approach that has shown promise is the use of reflected ultrasound. This make use of the fact that ultrasound will be

transmitted through a rough surface interface where there is asperity to asperity contact and be reflected where there are small air pockets. Thus a scan of reflected ultrasound across an interface can be achieved. A map of reflection coefficients can be generated, which can be converted to a contact pressure via a calibration process. This approach has been used successfully to study static wheel tread /rail head interfaces [4,5], but cannot be easily used on the flange because of the more complex geometry and is no use for field measurements.

In this work the information that can be obtained from a single stationary transducer has been explored, particularly looking at the flange contact. This was with a view to mounting a transducer on a wheel to provide dynamic sensing of flange contact. This could provide important information on where on a rail network, wear and RCF may be a problem.

At this early stage laboratory based tests have been carried out to determine the feasibility of detecting flange contacts.

## BACKGROUND

When an ultrasonic pulse strikes an interface between two materials it is partially transmitted and partially reflected. The proportion reflected, known as the reflection coefficient,  $R$ , depends on the acoustic impedance mismatch between the two materials according to equation (1). The ratio of the amplitude of the reflected wave to the amplitude of the incident wave, known as the reflection coefficient,  $R$ , is determined by:

$$R = \frac{z_1 - z_2}{z_1 + z_2} \quad (1)$$

where  $z$  is the acoustic impedance (the product of density and wave speed) of the media and the subscripts refer to the two sides of the interface.

The impedance of air and steel are 1.504 and 46.02 kg/m<sup>2</sup> μsec respectively. Thus when the pulse strikes a steel air interface ( $z_1 \gg z_2$ ) it is virtually all reflected and  $R=1$ . If the wave strikes a steel-steel interface and there is perfect contact, then it will be fully transmitted ( $z_1=z_2$ ) and  $R=0$ .

In practice wheel and rail surfaces are rough and when they are pressed together only a proportion of the geometrical (or nominal) contact area is actually in real contact. The interface consists of asperity contact regions and air gaps. This means that a complete interface between the two metal surfaces is practically impossible and  $R$  is always less than one. More detail on the relationship between the reflection coefficient and the rough surface contact conditions can be found in references [6-9].

An ultrasonic ray has a finite beam width and equation (1) is only valid if all the pulse strikes the interface normally. If some of the pulse misses the contact then the signal will be partially reflected.

Thus, in practice the reflection coefficient will vary from  $0 < R < 1$  depending both on whether the ray strikes the interface and on the conformity of the two contacting surfaces. The latter aspect (the effect of roughness and contact pressure on

reflection) can be handled analytically (see for example reference [7]). However the interaction of an ultrasonic ray with two complex shaped bodies in intermittent contact is more difficult. This paper is limited to a laboratory based experimental study of reflection from the wheel-rail contact. The objective is to establish whether measurement of reflection coefficient is sensitive to changes in flange contact.

Figure 1 shows the concept. A transducer is bonded onto the wheel at a predetermined orientation. The transducer is located either on a boss fixed to the wheel side, or in a shallow recess. The transducer emits ultrasonic pulses continuously. The pulses reflect from the flange region and are received by the same transducer (pulse-echo mode). Changes in the flange contact will alter the proportion of the wave transmitted into the rail and hence that reflected back to the transducer.

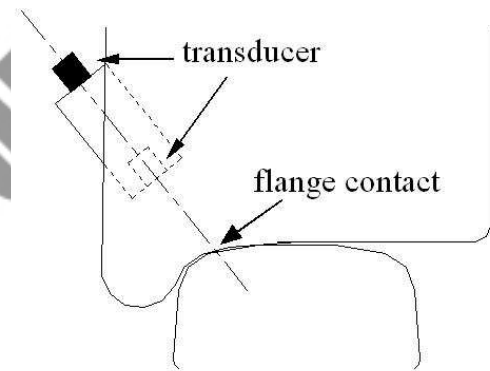


Figure 1. Schematic layout of an ultrasonic transducer located on a wheel (either mounted on a boss or within a small machined recess).

## APPARATUS & PROCEDURE

### Wheel and Rail Specimens and Loading

The wheel and rail specimens used in the experimental work were cut from sections of UIC 60 900A rail steel and R8T wheel steel (shown in Figure 2). The specimens were from used sections of rail, and exhibited some minor wear and surface polishing. The upper wheel specimen has had a flat surface machined at 47° degrees to the wheel axis. The transducer was coupled to this flat surface with a gel based couplant. The transducer was moved around on the face until a maximum reflection was achieved. The orientation of the plane (47°) was chosen to maximize the line of site between the transducer and the flange contact zone.



Figure 2. Photograph of the wheel and rail test specimen in contact.

A frame and two hydraulic cylinders shown in Figure 3 were used to normally and tangentially load the specimens together.



Figure 3. Photograph of the loading frame, showing the two hydraulic cylinders for applying normal and lateral loads.

Normal forces, varying from 0 to 80 kN in the vertical direction, were applied using an Enerpac hydraulic cylinder which was located below the wheel/rail specimens. Another hydraulic cylinder was used to generate lateral forces from 0 to 9 kN in the horizontal direction. As the wheel/rail components had no constraint in the horizontal direction, lateral force would cause relative sliding between wheel and rail. A large enough normal load must be applied to prevent this sliding. Applying a lateral load of more than 9 kN to a contact under a load of 80 kN caused gross slip to occur. The coefficient of friction was somewhere in the region of 0.1 to 0.12.

### Ultrasonic Instrumentation

Figure 4 shows a schematic of the ultrasonic instrumentation layout. The equipment consisted of an ultrasonic pulse receiver (UPR), oscilloscope, data processing computer and transducer. A principal part of the ultrasound apparatus is the UPR. This provides a voltage pulse which excites the transducer to produce an ultrasonic pulse. A conventional Panametrics 2 MHz contact transducer was used. The transducer consists of a piezo-electric element that converts the voltage pulse to a mechanical displacement pulse. This

travels through the wheel specimen, is reflected at the wheel/rail interface and received by the same transducer. The transducer outputs a small voltage which is passed to the UPR and amplified. The transducer was pulsed at 20 kHz; any faster than this and the reflected signal from one pulse tend to interfere with the next incident pulse.

The oscilloscope was used to digitize the received signal and download it to the computer. Multiple echoes are observed from other internal reflection within the wheel rail assembly. The reflection from the wheel-rail contact is extracted from the reflected pulse for further processing. LabVIEW was used to control the UPR and carry out signal processing.

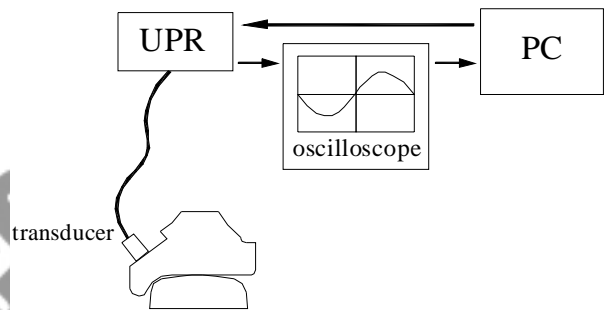


Figure 4. Schematic of the ultrasonic instrumentation.

### Signal Processing

Normal and lateral loads were applied in sequence. For each load case the reflected ultrasonic signal was captured and stored on the PC. The stored data was in the form of a voltage amplitude time domain signal.

Initially a reference amplitude is recorded when the wheel and rail are out of contact. In this case the ultrasound is reflecting from steel-air interface so  $R=1$  and all the wave amplitude is reflected. The reference reflected signal is then equal to the incident signal. All subsequent reflections are divided by this reference signal to give the reflection coefficient. The reflection coefficient amplitude is recorded. In practice it is easier to pass the time domain pulse through a Fast Fourier Transform (FFT) to obtain a reflection coefficient spectrum. The amplitude is easily obtained from this spectrum. The reflection coefficient amplitude was determined for each normal and lateral load combination.

### RESULTS

Figure 5 shows a series of reflected amplitude spectra for various applied normal loads. To obtain each of these curves the pulse reflected from the contact (i.e. amplitude in the time domain) has been passed through an FFT.

From the graph it can be seen that the transducer has a centre frequency of 2.2 MHz and a bandwidth of around 1.1 to 3.6 MHz.

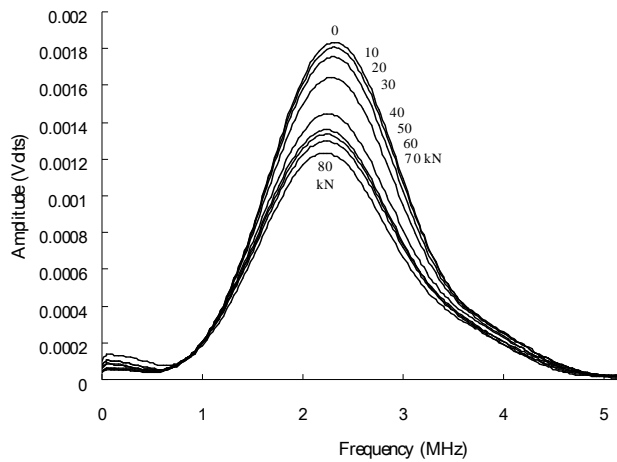


Figure 5. Pulses reflected from the wheel rail contact for range of normal loads. The pulses are presented as spectra in the frequency domain.

The pulse at zero applied load represents the case that has been fully reflected ( $R=1$ ). If each of the subsequent load pulses of Figure 5 is divided by the zero load case then the reflection coefficient spectrum is obtained. It is convenient to choose the reflection coefficient at the transducer centre frequency.

Figure 6 shows the reflection coefficient for increasing normal load and Figure 7 for increasing lateral force with normal load set at 80 kN.

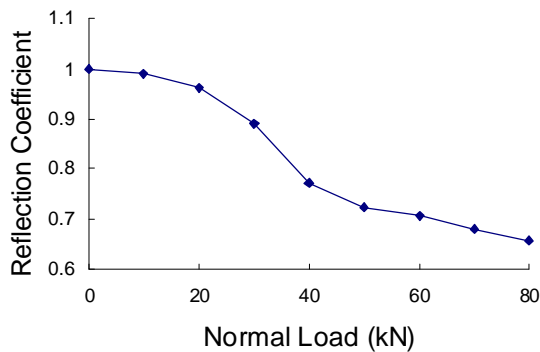


Figure 6. Measured reflection coefficient with increasing normal load.

The transducer is sensitive to changes in the normal load. There is probably a small amount of contact in the flange region and this is allowing some transmission of the sound wave. As the lateral force is increased the signal drops even further as the size and extent of the flange contact region grows.

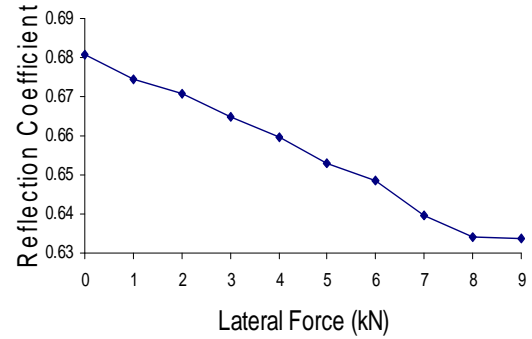


Figure 7. Measured reflection coefficient with increasing lateral load, whilst the normal load is fixed at 80 kN.

In further tests, series lateral as well as normal loads were applied to the specimens. Figure 8 shows a map of the measured reflection coefficient as it varies with normal and lateral loads.

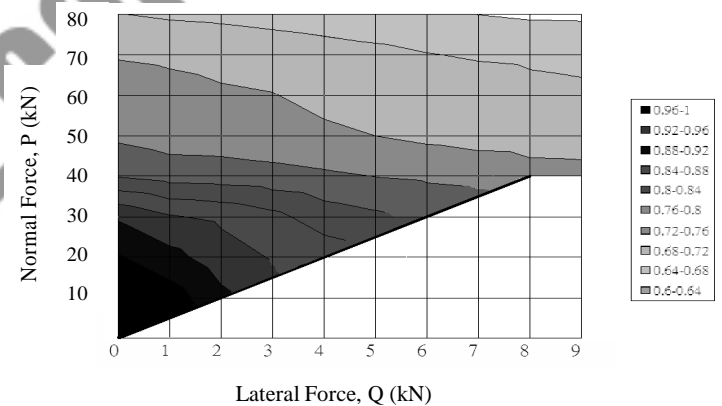


Figure 8. Map of reflection coefficient variation with normal and lateral load.

### Inked Paper to Visualize the Contact

To help establish the location of the contact region, some simple tests were performed with carbon paper pressed in between the wheel and rail. Figure 9 showed the results under different lateral loads. The pictures clearly show a tread contact region – which appears to be fragmented into two distinct regions; and a flange contact. The flange contact grows as the lateral load is increased.

These images are likely to be an over-estimate of the real contact patch as the thickness of the paper is likely to bridge the gap between some non-contacting regions of the wheel and rail. Also they will show the total loading history. Thus if the application of a lateral force causes an unloading of the head contact region only the maximum contact area and not the loading end point contact area will be displayed.

Nevertheless they show that the flange contact region is increasing with lateral load. It would be expected that this would cause a reduction in the reflection coefficient, as observed in figures 7 and 8.

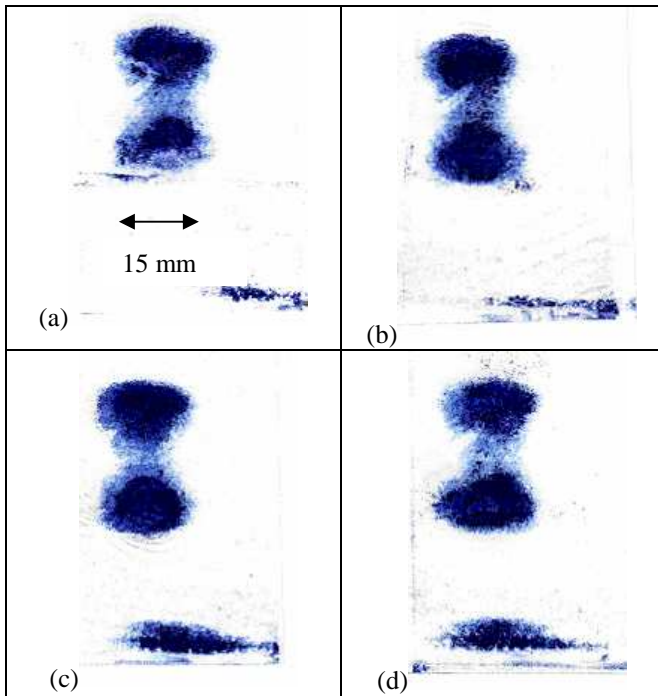


Figure 8. Carbon paper image of the wheel rail contact under a normal load of 80 kN and a lateral load of; (a) 2 kN (b) 4 kN (c) 6 kN, and (d) 8 kN.

## DISCUSSION

The results have shown that a single ultrasonic transducer can be placed on the wheel and is sensitive to both increasing normal load and lateral load. The map shown as figure 8 demonstrates that there is enough sensitivity to deduce whether flange contact is occurring and the level of the lateral load. It is theoretically possible for the rail to make contact at any wheel location from the flange throat to the flange face. In this work only locations at the throat have been studied and at this stage the range of possible positions that can be measured has not been identified. A more detailed study of the transducer location could both improve the sensitivity of the measurements and define what flange contact positions are best observed. Further work will be carried out to model the ultrasonic ray passage through the combined wheel-rail assembly in a wider range of configurations to ensure the best location is chosen.

However, this has been an entirely laboratory based static study. There are two main issues that arise when transferring the concept to the field. The first is that the transducer is mounted on a rotating component. The second is that both because of this rotation, and also the dynamics of the wheel-set, flanging contact will be a transient phenomenon with respect to the transducer location.

Mounting the transducer on a rotating wheel should not prove difficult. The pulsing and receiving apparatus could be mounted on the vehicle and slip rings used to transmit the voltage pulses. This kind of approach has been used when

measuring from the shaft of a large size journal bearing [10] without difficulty. Alternatively small scale pulsers and receivers are commercially available (and are used extensively in liquid pipe flow measurement). It would be possible to mount such a device on the wheel, process the data on board, and send the resulting amplitude data via telemetry.

The possibility of recording a transient contact signal is more pertinent. The pulsing rate was set at 20 kHz, or one pulse every 50  $\mu$ s. In principle, provided the sensor is in position, events occur at that time interval can be observed. If the train speed is 120 km/h the contact patch will have moved 1.65 mm in the time between two consecutive pulses. It should be possible therefore, to record 10 to 15 pulses from a contact patch (say 20 mm in diameter) whilst the sensor moves over the patch as the wheel rotates. It is also possible to trigger the sensor so it is designed to pulse exactly when the contact is immediately beneath the sensor location (this procedure has been validated on measurements from ball bearing contacts in reference [11]). Clearly if flange contact is intermittent and associated with an irregularity on the wheel then the sensor may or may not pick this up depending on its location with respect to the irregularity.

## CONCLUSIONS

A feasibility study has been carried out to determine whether a wheel mounted ultrasonic sensor can be used to determine whether flange contact is occurring in a wheel-rail contact. Specimens were cut from sections of wheel and rail and were loaded together whilst measurements of ultrasonic reflection were carried out.

The reflection coefficient was seen to fall from 1 to 0.68 as the normal load was increased from zero to 80 kN. As the lateral load was increased to 9 kN, at this maximum normal load, the reflection coefficient dropped to 0.63. In this way, the reflection was sensitive to both normal and lateral loads. An experimental map of this relationship has been created.

It is potentially feasible to deduce whether flange contact is occurring and also estimate what the normal and lateral loads are. Adapting this approach to the field will require consideration over the position of pulsing equipment, and the relationship between the pulsing rate and the transient nature of the flange contact expected.

## REFERENCES

- [1] Lewis, R. and Dwyer-Joyce, R.S., 2006, "Wheel/Rail Tribology", in Totten, G.E., editor, Handbook of Lubrication and Tribology: Volume 1 - Application and Maintenance, Second Edition, CRC Press.
- [2] Pau, M., Aymerich, F., Ginesu, F., 2001, "Measurements of nominal contact area in metallic surfaces: a comparison between an ultrasonic method and a pressure sensitive film", Wear, Vol. 249, pp. 533-535.

- [3] Poole W., 1987, "The Measurement of Contact Area between Opaque Objects under Static and Dynamic Rolling Conditions", *Proceedings of Contact Mechanics and Wear of the Wheel/rail System*, University of Rhode Island, Waterlooville Press, pp59-72.
- [4] Pau, M., Aymerich, F., Ginesu, F., 2000, "Ultrasonic Measurement of Nominal Contact Area and Contact Pressure in a Wheel/Rail System", *Proceedings of the IMechE Part F, Journal of Rail and Rapid Transit*, Vol. 214, pp231-243.
- [5] Marshall, M.B., Lewis, R., Dwyer-Joyce, R.S., Olofsson, U., Bjorklund, S. 2006, "Experimental Characterisation of Wheel-Rail Contact Patch Evolution", *ASME Journal of Tribology*, Vol. 128, No. 3, pp. 493-504.
- [6] Nagy, P.B., (1992) Ultrasonic classification of imperfect interfaces, *Journal of Non-destructive Evaluation*, Vol. 11, Nos. 3/4, 127-139.
- [7] Drinkwater, B. W., Dwyer-Joyce, R. S. and Cawley, P., A study of the interaction between ultrasound and a partially contacting solid-solid interface, *Proceedings of the Royal Society of London A*, 452, 2613-2628 (1996).
- [8] Baltazar, A., Rokhlin, S., and Pecorari, C., (2002), 'On the Relationship between Ultrasonic and Micromechanical Properties of Contacting Rough Surfaces', *Journal of the Mechanics and Physics of Solids*, Vol. 50, pp. 1397-1416.
- [9] Dwyer-Joyce, R. S., Drinkwater, B. W., and Quinn, A.M., (2001), "The Use of Ultrasound in the Investigation of Rough Surface Interfaces", *ASME J. Tribology*, Vol. 123, pp. 8-16.
- [10] Kasolong, S. and Dwyer-Joyce, R.S., (2008), Observations of the Film Thickness Profile and Cavitation Around the Circumference of a Journal Bearing, in press *STLE Tribology Transactions*.
- [11] Zhang, J, Drinkwater, B.W., and Dwyer-Joyce, R.S., (2005), Acoustic Measurement of Lubricant Film Thickness Distribution in Ball Bearings, *The Journal of the Acoustical Society of America*, Vol. 119, issue 2, pp. 863-871.